ISSN (e): 2250 – 3005 || Volume, 06 || Issue, 6|| June – 2016 ||
International Journal of Computational Engineering Research (IJCER)

Analysis of an Evaporative Inlet Air Cooled Combined Cycle for Propulsive Systems in Ships

DrAlok Kumar Mohapatra[1],Deepak Kumar Hota[2] ,Prajna Acharya[3]

[1] *Professor, Department of Mechanical Engineering, Gandhi Institute For Technology (GIFT), Bhubaneswar*
[2] *Assistant Professor, Department of Mechanical Engineering, Gandhi Engineering College, Bhubaneswar*
[3]*Assistant Professor, Department of Mechanical Engineering, Gandhi Institute For Technology (GIFT), Bhubaneswar*

Abstract
The integration of inlet air cooling to gas turbine based power utilities is a well accepted practice as this modification to the utility delivers superior utility performance. However, application of inlet-air cooling to drive turbines and specifically to marine mobility sector is rare in literature. Marine vessels are generally propelled by diesel engines, however large marine vessels specifically cruise ships and high speed naval vessels may have requirements of higher speeds and on-board power requirements which can fulfilled by gas turbine driving the propellers while on-board power needs can be met by steam turbine power generated from gas turbine exhaust heat. Such gas-steam combined cycles have the potential to become popular for high capacity marine vessels. The choice of gas turbine based combined cycle power plant for marine vessels in comparison to diesel engine powered vessel is also superior due to lower emission from the former. Higher ambient temperatures are known to negatively affect gas turbine and hence also marine combined cycle performance. The present article discusses the prospects of using an evaporative inlet air cooled combined cycle as a prime mover for marine application. A parametric study of the effect of compressor pressure ratio, turbine inlet temperature, ambient relative humidity and ambient temperature on energy, exergy and emission performance of combined cycle used in marine application has been carried out. Evaporative inlet cooling integrated to cooled gas-turbine based combined-cycle has been observed to improve the power output by 10.39 % and efficiency by 1.21 %. This improvement has been observed to be higher at higher ambient temperature and lower ambient relative humidity. Inlet air cooling has also observed to improve emission performance with lower NOX and CO emission. The overall cycle exergy destruction has also been observed to reduce due to the addition of inlet air cooling to a gas turbine propelled/powered based combined cycle.

I. INTRODUCTION

Majority of prime movers for ship propulsion used currently are diesel engines primarily because of their higher efficiency (even at part load) and their ability to run on residual oil. However in view of the increasing awareness for pollution control and stricter environmental regulations, combined cycle can be regarded as a suitable alternative to propel large ships for cargo and military purpose [Eyring 1]. Also in case of combined cycle the power density is higher and so the requirement of space is lower as compared to diesel engines. This additional space can be utilized to increase the seating capacity in ships. A comparative study by … on a 2500 passenger ship reveals that the seat capacity can be increased by 2.5 % and power requirement can be reduced by 1.5 % if a combined cycle is used as a prime mover instead of traditional diesel engines

[Alvarez 2]. There is published literature on the effect of compressor inlet cooling on gas-turbines and combined-cycle plants. Chaker and Homji [3] discussed the impact of incorporating a media evaporative cooler to gas-turbine engines and suggested methods to improve reliability. A detailed review of evaporative cooling has been presented in terms of the thermodynamics and technological aspects of analysis. The theory application of wetted rigid media evaporative coolers integrated to industrial gas-turbines has been discussed in detail by Johnson [4]. A detail discussion on design, operation and installation has been carried out in addition to the evaluation of performance parameters of evaporative cooler. The effect of inlet fogging integrated to a combined cycle power plant studied by Chiang et al. [5] and shows an increase in power in the range of 1.9% to

16.87% which depends on the percentage of overspray. An extensive study of effect of inlet air cooling schemes on gas turbines and combined cycle is performed by Mohapatra et al. [6-9]

Application of inlet-air cooling to drive turbines and specifically to marine mobility sector is rare in literature. A detailed review on use of gas-steam combine cycle as a prime mover for ship is performed by haglinds. The performance evaluation of a combined cycle used in cruice ship applications is discuseed by E Douglas 10. Cycles with integrated electric propulsion systems were evaluated in various combinations of diesel engines, gas turbines and steam turbines for ship power plants. The Thermoeconomic investigation of different gas turbine configuration for marine applivcation is carried out by Kumar et al 11. The plant cost (including equipment purchase cost, fuel cost, maintenance and investment cost) for proposed configurations of gas turbine cycles has been calculated and presented

…. 12 Has considered the combined cycle as the future of ship propulsion and reported that.Sinhaet 13. al. have investigated relative merit of different propulsion options for large ships. None of the published literature has discussed the application of inlet-air cooling to drive turbines and specifically to marine mobility sector. The gas turbine output as well as efficiency strongly dependson the ambient temperature. A gas turbine loses approximately 7% of its nominal power when the intake temperature increases from 15^0 C, ISO conditions, to 25^0 C. During summer, the ambient temperature increases above the 25^0 C, the losses are still bigger, reaching even 15% of the power rating at 36^0 C [14]. In such conditions, power augmentation should be essentially carried out. In hot and dry air regions, gas turbine power output is dramatically reduced because of the reduction in gas turbine air mass flow. This effect is particularly predominant with aero derivative units that are commonly used in the marine drive. Domachowski and Dzida 15 studied the effect of evaporative inlet cooling on marine gas turbines. Different areas of ship's voyage have been taken into account and potential power gain has been calculated. The present article analyses the effect of integration of evaporative inlet air cooling to a marine gas-steam combined cycle system. Energy, Exergy and Emission analysis of a single pressure HRSG combined cycle used for marine application is carried out and results presented.

II. COMPONENT MODELING AND GOVERNING EQUATIONS

Figure 1 show the schematic diagram of a gas-turbine single pressure HRSG combined-cycle with evaporative inlet cooling and air film bucket cooling system. Component-wise modeling of the EV1PR is as under:

2.1 Gas Model

In the present model the specific heat of gas is assumed to vary only with temperature in the form of polynomials as follows [25].

(1 a)

$$c_{pg}(T) = f_h * \left[0.991 + \left(\frac{6.997T}{10^5} \right) + \left(\frac{2.712T^2}{10^7} \right) + \left(\frac{6.997T^3}{10^{10}} \right) \right]$$ where f_h is the humidity correction factor to account for the effect of increase in specific humidity of ambient air across the air-humidifier

$$f_h = 1 + 0.05\phi_{h,e} \quad (1\text{ b})$$

where $\phi_{h,e}$ is the relative humidity at the outlet of humidifier.

$$h = \int_{T_a}^{T} c_p(T)dT \quad (2)$$

Here all non-reacting components of air are arbitrarily assigned zero value of enthalpy at ambient pressure and temperature (inlet of IAC). This is because the ambient condition is the dead state above which work potential of working fluid is determined. For thermodynamic study, the fuel composition taken into account is CH_4= 86.21 %, C_2H_6= 7.20 %, and CO_2= 5.56 %, and N_2 = 1.03 % by weight.

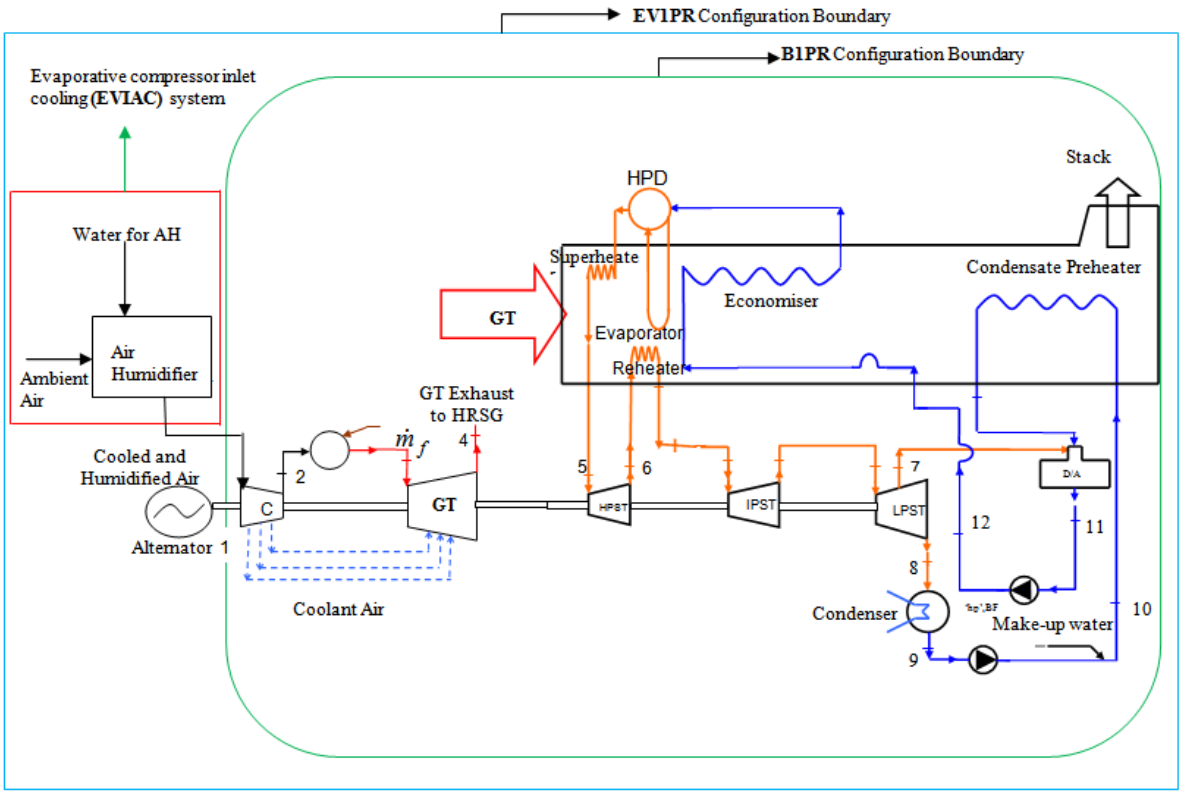

Figure 1 Schematic of a simple gas single pressure reheat steam cycle with and without evaporative cooling of inlet air (EV1PR) configuration

2.2 Humidifier Model

Cooling in hot, relatively dry climate can be accomplished by evaporative cooling. Evaporative cooling involves passing air across a spray of water or forcing air through a soaked pad that is kept replenished with water [26]. Owing to the low humidity of entering air, a part of the water injected evaporates. The energy required for evaporation is provided by the air stream, which undergoes a reduction in temperature. The following assumptions are made in the humidifier model.

- The relative humidity at the humidifier outlet is 95%
- The pressure drop of air in the humidifier is 1% of the ambient air pressure.

Applying the mass balance equation across the humidifier control volume boundary gives

$$\omega_{a,e} = \omega_{a,i} + m_w \tag{3}$$

where ω is the specific humidity and is calculated at a certain temperature as

$$\omega = \frac{0.622 p_{vap}}{p - p_{vap}} \tag{4}$$

where $p_{vap} = \phi p_{sat}$ is the partial pressure of vapor, ϕ is the relative humidity and p_{sat} is the saturation pressure of air corresponding to the desired temperature.

The energy balance equation for the humidifier is given by

$$h_{a,e} = h_{a,i} + (\omega_{a,e} - \omega_{a,i}) h_w \tag{5}$$

Where $h_{a,e}$ and $h_{a,i}$ are the enthalpy of moist air at outlet and inlet of the air humidifier respectively and are calculated as follows

$$h_{a,e} = c_{p,a,e} t_{a,e} + (2500 + 1.88 t_{a,e}) \omega_{a,e} \tag{6a}$$

$$h_{a,i} = c_{p,a,in} t_{a,i} + (2500 + 1.88 t_{a,i}) \omega_{a,i} \tag{6b}$$

$$T_{a,e} = t_{a,e} + 273 \tag{6c}$$

The equations (3 – 6) has been solved to determine the value of $T_{a,e}$, $\omega_{a,e}$ and m_w.

2.3 Compressor Model

The compressor used in gas-turbine power plant is of axial flow type. The thermodynamic irreversibilities in an axial flow compressor are incorporated in the model by introducing the concept of polytropic efficiency.

Reference [23] gives detail discussion on modeling and governing equations.

Using mass and energy balance across control volume of compressor, the compressor work is calculated as follows:

$$\dot{m}_{comp,i} = \dot{m}_{comp.e} + \sum \dot{m}_{coolant,j} \tag{7}$$

$$\dot{W}_{comp} = \dot{m}_{comp,e}.h_{comp,e} + \sum \dot{m}_{coolant,j}.h_{coolant,j} - \dot{m}_{comp,i}.h_{comp,i} \tag{8}$$

2.4 Combustor Model:

For given values of turbine $T_{i,T}$, pressure drop and combustion efficiency, the fuel flow is found from the mass and energy balance,given by,

$$\dot{m}_e = \dot{m}_i + \dot{m}_f \tag{9}$$

$$\dot{m}_f \cdot \Delta H_r \cdot \eta_{comb} = \dot{m}_e \cdot h_e - \dot{m}_i \cdot h_i \tag{10}$$

The combustion reaction and the combustion products of hydrocarbon fuel ($C_{a1}H_{b1}$) are expressed as

$$\begin{aligned} &C_{x_1}H_{y_1} + \xi \cdot \left(x_{o_2}O_2 + x_{N_2}N_2 + x_{H_2O}H_2O + x_{CO_2}CO_2\right) \\ &\rightarrow \xi \cdot \left(y_{CO_2}CO_2 + y_{N_2}N_2 + y_{o_2}O_2 + y_{H_2O}H_2O\right) \end{aligned} \tag{11}$$

Where

$$y_{CO_2} = \frac{x_1}{\xi} + x_{CO_2} \tag{12}$$

$$y_{N_2} = x_{N_2} \tag{13}$$

$$y_{H_2O} = \frac{y_1}{2\xi} + x_{H_2O} \tag{14}$$

$$y_{O_2} = x_{CO_2} - \frac{x_1}{\xi} - \frac{y_1}{4\xi} \tag{15}$$

$$\xi = \frac{n_a}{n_f} \tag{16}$$

2.5 Cooled Gas-turbine model

In this work, the gas-turbine buckets have been modeled to be cooled by air-film cooling (AFC) method. The cooling model used for cooled turbine is the refined version of that by Louis et al [14]. The mass flow rate of coolant required in a bucket row is expressed as [27]:

$$a_{coolant} = \frac{\dot{m}_{coolant}}{\dot{m}_g} = \left[\frac{Sn_{in} \cdot c_{p,g}}{\varepsilon \cdot c_{p,coolant}}\right] \times \left[\frac{S_b \cdot F_{sa}}{t \cdot \cos\alpha_{mean}}\right] \times \left[\frac{T_{g,i} - T_b}{T_b - T_{coolant,i}}\right] \tag{17}$$

where $S_b \cong 2c$, $S_b/t\cos\alpha_{mean}=3.0$, $F_{s,a} = 1.05$, $\alpha_{mean} = 45°$ (for stator), $\alpha_{mean} = 48°$ (for rotor), $Sn_{in}=0.005$.

Turbine power is given by the mass and energy balance of gas-turbine as under:

$$\dot{W}_{gt} = \left[\dot{m}_{g,i} \cdot (h_{g,i} - h_{g,e})\right] + \left[\sum \dot{m}_{coolant} \cdot (h_{coolant,i} - h_{coolant,e})\right] \tag{18}$$

2.6 HRSG Model

In the present study, the bottoming cycle employs an unfired triple pressure HRSG with reheat (3PR). The selection of steam pressure and temperature for 3PR system is based on the optimized value to yield maximum steam cycle efficiency satisfying the minimum stack temperature and quality of steam at 'lp' turbine exhaust. Reference [28] outlines the detailed procedure.

2.7 Steam-turbine model

Exhaust gas extracted at an appropriate point prior to the exit of HRSG having sufficient heat energy, is supplied to the VA generator such that:

$$\dot{m}_{g,hrsg,i} = \dot{m}_{g,hrsg,e} + \dot{m}_{g,gen,i} \tag{27}$$

The amount of steam produced in HRSG reduces due to the extraction of this exhaust gas from it which results in a reduction of steam-turbine work.

Mass and energy balance yield steam-turbine output given by,

$$\dot{W}_{st} = \sum^{stages} \dot{m}_{s.i} \cdot \left(h_{s,i} - h_{s,e}\right) \tag{28}$$

$$h_{s,i} - h_{s,e} = \eta_{st} . \left(h_{s,i} - h_{s,e}\right)_{isentropic} \tag{29}$$

2.8 Condenser model

The mass and energy balance give the cooling requirement as below.

$$\dot{m}_{s,d/a,i} + \left(\dot{m}_{cond} - \dot{m}_{s,d/a,i}\right) = \dot{m}_{s,d/a,e} \tag{30}$$

$$\dot{m}_{s,d/a,i} . h_{s,d/a,i} + \left(\dot{m}_{cond} - \dot{m}_{s,d/a,i}\right) h_{s,cond,e} = \dot{m}_{s,d/a,e} . h_{s,cond,e} \tag{31}$$

2.9 De-aerator model

The mass and energy balance give the amount of steam extracted for deaeration

$$\dot{m}_{s,d/a,i} + \left(\dot{m}_{cond} - \dot{m}_{s,d/a,i}\right) = \dot{m}_{s,d/a,e} \tag{32}$$

$$\dot{m}_{s,d/a,i} . h_{s,d/a,i} + \left(\dot{m}_{cond} - \dot{m}_{s,d/a,i}\right) h_{s,cond,e} = \dot{m}_{s,d/a,e} . h_{s,cond,e} \tag{33}$$

Inside the deaerator $\dot{m}_s$ is in liquid form.

2.10 Pump model

The mass and energy balance yields the pump work input needed:

$$\dot{m}_{w,i} = \dot{m}_{w,e} \tag{34}$$

$$\dot{w}_p = \sum v_{w,i} . \left(p_e - p_i\right) \tag{35}$$

2.11 Thermo-environmental model

The reduction of CO_2 emissions from the cycle is related to the adoption of advanced thermodynamic characteristics of cycle components like the compressor and gas-turbine isentropic efficiency which results in higher purchase cost of each component in the cycle. The environmental impact is expressed here as the total cost rate of pollution damage (\$/h) due to CO_2 emission (C_{env,CO_2}) by multiplying its flow rates by corresponding unit damage cost, which have been reported elsewhere as, C_{CO_2} = 0.024\$/kg [25]. In the present work the cost of pollution damage is assumed to be added directly to other system costs.

The CO_2 emission per unit plant output is given as:

$$\kappa = \frac{\dot{m}_{CO_2} \times HR}{LHV} \frac{kg}{kWh} \tag{27}$$

Where $\dot{m}_{CO_2}$ = mass of CO_2 produced in kg per kg fuel.

Cost rate of environmental impact due to CO_2 emission

$$C_{env,CO_2} = \dot{m}_{CO_2} \times \dot{m}_f \times C_{CO_2} \ \$/\text{h} \tag{28}$$

Where $\dot{m}_f$ = mass of fuel supplied in kg per hour.

III. PERFORMANCE PARAMETERS:

The general expressions to calculate the performance parameters for gas-turbine and combined-cycle plant are given as follows:

The gas cycle power ($\dot{W}_{gc}$) is given by

$$\dot{W}_{gc,net} = \dot{W}_{gt} - \frac{\left|\dot{W}_c + \dot{W}_{ref}\right|}{\eta_m} \tag{38}$$

The steam cycle power ($\dot{W}_{sc,net}$) is given by:

$$\dot{W}_{sc,net} = \dot{W}_{st}.\eta_m - \frac{\left|\dot{W}_p\right|}{\eta_p} \tag{39}$$

where 'η_p' is the overall pump efficiency and '$\dot{W}_p$' is pump power

The combined-cycle power (W_{plant}) is given by:

$$\dot{W}_{plant} = \dot{m}.\dot{w}_{plant} = \eta_{alt}.\left[\dot{W}_{gc,net} + \dot{W}_{sc,net}\right] \tag{40}$$

The combined-cycle plant efficiency (η_{plant}) is expressed as:

$$\eta_{plant} = \frac{\dot{W}_{plant}}{\dot{m}_f \cdot \Delta H_r} \tag{41}$$

Another parameter of great importance to the gas-turbine is the work ratio [29]

$$\dot{W}_{rat} = \frac{\dot{W}_{gt}}{\left|\dot{W}_c\right|} \tag{33}$$

This parameter should be as large as possible, because a large amount of the power produced by the turbine is required to drive the compressor, and because the engine net work depends on the excess of the turbine work over the compressor work.

Heat Rate (HR) is the rate of heat input (kJ/h) required to produce unit power output (1kW).

$$HR = \frac{3600\,Q \times m_a}{\dot{W}_{plant}} = \frac{3600}{\eta_{plant}} \quad \left(\frac{kJ}{kWh}\right) \tag{34}$$

Modeling of cycle components and governing equations developed for cycles proposed above have been coded using C++ and results obtained. The input data used in the analysis is given in Table 1.

IV. RESULTS AND DISCUSSION

In the present study the environmental impact in terms of CO_2 emissions has been integrated with the energetic analysis of a evaporative compressor inlet cooled FC3PR combined-cycle through the help of performance curves, plotted using modeling, governing equations and input parameters (Table1).

It is assumed that the volumetric composition of the inlet air is 0.7567 N_2, 0.2035 O_2, 0.003 CO_2 and 0.036 H_2O. To improve environmental sustainability, it is necessary not only to use sustainable or renewable sources of energy, but also to utilize non-renewable sources like natural gas fuel more efficiently, while minimizing environmental damage. In this way, society can reduce its use of limited resources and extend their lifetime. CO_2 accounts for about 50% of the anthropogenic greenhouse effect. A major energy efficiency program would provide an important means of minimizing greenhouse effect through reduced CO_2 emission.

The gas-turbines are designed to operate at ISO condition (T_{amb} = 15° C and RH_{amb} = 0.6). But in the present article the $T_{i,C}$ and RH_{amb} has been varied and ISO condition is not achieved at all times. However the

results obtained in this article have been validated with the characteristics of MS 7001 gas-turbine from General Electric [7, 32] under off design conditions and with compressor inlet cooling and is found to compare well.

4.1 Effect of T_{amb} *and* RH_{amb} *on mass of bucket coolant and mass of water added in the humidifier*

Fig 2 depicts the variation of mass of bucket coolant and mass of water added in the humidifier w.r.to T_{amb} and RH_{amb}. It is observed that as T_{amb} decreases, the mass of water vapor added in the humidifier decreases due to lower difference between DBT and WBT. However the bucket coolant mass also reduces due to reduction in $T_{i,C}$ As RH_{amb} reduces, there is an increase in mass of water vapor picked up by the humidifier as shown in the figure which results in a corresponding increase in temperature drop achieved across the humidifier and mass of bucket coolant required reduces proportionately.

4.2 Effect of $T_{i,T}$ *and* β_{comp} *on requirement of coolant flow.*

Fig 3 shows the requirements of coolant flow rates with variation in $T_{i,T}$ and compressor pressure ratio. It can be seen that the coolant flow rate increases significantly with increase in $T_{i,T}$ in order to maintain the turbine bucket temperature within specified limits. However, the variation in cooling flow rates with change in β_{comp} is not appreciable rather monotonous. This is because of the fact that increase in β_{comp} has no significant affect on the bled air coolant temperature.

4.3 Variation of $\dot{w}_{plant}$ *and* η_{plant} *with* $T_{i,T}$ *for FC3PR cycles with and without evaporative compressor inlet cooling*

Fig. 4(a) shows the variation of $\dot{w}_{plant}$ with $T_{i,T}$ for FC3PR cycles with and without evaporative compressor inlet cooling. It is observed that with increase in $T_{i,T}$, the $\dot{w}_{plant}$ of all cycle configurations initially increases, the rate of increase being higher at lower value of $T_{i,T}$. The relative increase in $\dot{w}_{plant}$ of EVFC3PR cycle over FC3PR is observed to be higher at elevated $T_{i,T}$. This is because at elevated $T_{i,T}$,the increase in turbine specific work outperforms the increase in pumping, cooling and mixing irreversibilities, which is always positive and the net gain is higher at lower values of $T_{i,T}$. This is because at higher $T_{i,T}$ the bucket coolant requirement increases and so the effectiveness of compressor inlet cooling also increases proportionately.

Fig. 4(b) shows the variation of η_{plant} with $T_{i,T}$ for FC3PR cycle with and without evaporative compressor inlet cooling which signifies the importance of integrating compressor inlet cooling to a cooled gas-turbine based combined-cycles. The optimum η_{plant} in case of FC3PR cycle is observed to be 1650 K. This is because beyond a $T_{i,T}$ of 1650 K, the efficiency benefits of elevated temperatures may be more than compensated by the increased irreversibilities associated with the required cooling flow rates. This optimum temperature corresponding to maximum efficiency is increased to 1750 K for EVFC3PR configurations due to reduction in $T_{i,C}$ resulting in a subsequent reduction in temperature of coolant bled from the compressor. This ensures a higher $T_{i,T}$ to be adopted compared to non inlet cooled cycle and therefore higher η_{plant} is achieved.

4.4 Effect of evaporative inlet cooling and film bucket cooling on η_{plant} *and* $\dot{w}_{plant}$ *of B3PR cycle.*

Fig. 5 shows the effect of evaporative compressor inlet cooling and air film bucket cooling on performance of gas-turbine cycle at T_b=1123 K, β_{comp} =23, T_{amb} =313 K, RH_{amb}=0.2. It has been observed that the incorporation of air humidifier increases the $\dot{w}_{plant}$ and η_{plant} of B3PR cycle. This is due to lower compression work and increased mass flow rate of air due to increased density. Both of these factors increase $\dot{w}_{plant}$. The heat energy input also increases at lower $T_{i,C.}$ The increase in $\dot{w}_{plant}$ compensates the increase in fuel energy input well and thereby causes an increase in η_{plant} . Though there is sharp increase in fuel energy input with increasing $T_{i,T}$, it is well compensated by the increase in $\dot{w}_{plant}$ and hence an enhancement in η_{plant} results.

It is observed that the effect of evaporative compressor inlet cooling is superior in case of FC3PR cycle as compared to B3PR cycle. The incorporation of evaporative compressor inlet cooling increases the η_{plant} of B3PR cycle by 0.8 % and $\dot{w}_{plant}$ by 9.04 %, against 1.21 % and 10.39 % respectively for FC3PR cycle. This is

because, in case of FC3PR cycle, the addition of evaporative inlet cooling has the additional benefit of lowering the bucket coolant requirement and associated losses.

4.5 Effect of RH_{amb} *and* T_{amb} *on temperature drop* η_{plant} *and* $\dot{w}_{plant}$ *of evaporative inlet cooled combined-cycle*

Fig 6(a) shows the variation of temperature drop (achieved in the EVIAC) , η_{plant} and $\dot{w}_{plant}$ with respect to T_{amb} for EVFC3PR configuration. It is interesting to note that, as T_{amb} increases, the $\dot{w}_{plant}$ reduces in spite of an increase in temperature drop across the humidifier. This is because at higher T_{amb}, though the drop in temperature is higher, owing to higher difference between WBT and DBT, the $T_{i,C}$ is also higher. As the $T_{i,C}$ increases, the compressor work is increased along with the mass of bucket coolant required. Although the fuel consumption is reduced for a given $T_{i,T}$, the drop in gas-turbine work due to rise in mixing and cooling irreversibilities and the increase in compressor work due to higher $T_{i,C}$ together results in a net reduction in $\dot{w}_{plant}$ and η_{plant}.

Fig 6(b) shows the variation in η_{plant}, $\dot{w}_{plant}$ and the drop in temperature achieved across the humidifier with respect to RH_{amb}. Since the relative humidity at the outlet of humidifier is assumed constant, a lower RH_{amb} corresponds to a higher amount of water vapor picked up by the humidifier, as a result of which the temperature drop across the humidifier is increased and the effect of evaporative cooling is enhanced. This leads to lesser work of compression and lesser amount of bucket coolant requirement, which results in the enhancement of η_{plant} and $\dot{w}_{plant}$. This performance enhancement is also due to increase in the specific volume of working fluid (due to higher amount of water vapor added in the humidifier). The effect is similar to that observed in gas-turbine with water injection at compressor inlet. Also due to a reduction in compressor inlet air temperature, the temperature of coolant bleed-air gets reduced. This in turn reduces the bucket coolant requirement and hence lowers bucket coolant mixing irreversibilities which results in enhanced plant performance.

4.6 Variation of normalized CO_2 *emission with* $T_{i,T}$ *for FC3PR combined-cycle with and without EVIAC.*

Fig. 7 shows the effect of evaporative compressor inlet cooling and $T_{i,T}$ on CO_2 per unit plant output of 3PR combined-cycle. It has been observed that the compressor inlet cooled cycle has less CO_2 emission per unit plant output, than the cycle without compressor inlet cooling, which signifies the importance of incorporation of compressor inlet cooling in terms of enhanced plant performance and hence reduced environmental damage. The variation of per unit plant output of CO_2 emission with $T_{i,T}$ suggests that the CO_2 emission reduces rapidly with increase in $T_{i,T}$upto a certain optimum value. This optimum $T_{i,T}$ with reference to minimum normalized CO_2 emission is found to be 1650 K for FC3PR cycle and 1750 K for EVFC3PR cycle which also corresponds to the maximum efficiency. A higher value of $T_{i,T}$ can be adopted by adopting superior bucket cooling techniques. It can therefore be concluded that the collective effect of compressor inlet cooling and gas-turbine bucket cooling has a significant effect on sustainable development in terms of reduced green house gas emission.

4.7 Effect of β_{comp} *and ambient* λ_{IT} *on Heat rate and Work ratio of EVFC3PR cycle*

Fig 8 shows the effect of variation of β_{comp} and ratio of $T_{i,T}$ to $T_{i,C}$ on heat rate and work ratio. It can be observed that the work ratio increases with increase in λ_{IT} and decrease in $r_{p,\,c}$. The effect of variation of λ_{IT} on heat rate implies that with increase in β_{comp} the heat rate first decreases and than starts to rise. For a given β_{comp}, the heat rate is minimum for a specific value of λ_{IT}. This optimum value of λ_{IT} has been found out to be 5.6 at an β_{comp} of 20 and 6 at an β_{comp} of 28. The variation of heat rate with β_{comp} shows that at anλ_{IT} of 6.4, the heat rate decreases with increase in β_{comp}. As the value of λ_{IT} decreases this reduction in heat rate w.r.t β_{comp} gradually becomes less significant and below anλ_{IT} of 5.2 this trend is reversed and the heat rate increases with increase in β_{comp}. The optimum value of β_{comp} is found out to be 28 at an λ_{IT} of 6.4, while it is 16 at an λ_{IT} of 4.8. The existence of this optimum λ_{IT} and β_{comp} is due to the collective effect of various factors. With increase in both β_{comp} and λ_{IT}, the compressor work input, the fuel and bucket coolant requirement increases. The gas cycle work also increases, but is limited by increasing pumping, bucket cooling and mixing irreversibilities. The gas-turbine exhaust temperature rises with rise in λ_{IT} but drops with rise in β_{comp} which decides the steam generated in HRSG and hence the steam-turbine output.

The work ratio increases by 24.22% and heat rate reduces by 8.16% when λ_{IT} increases from 4.8 to 6.0 at an β_{comp} of 28. Similarly the heat rate reduces by 4.43% when the β_{comp} increases from 16 to 28 at anλ_{IT} of 6.4.

4.8 Variation of CO_2 *emission with* λ_{IT} *and* β_{comp} *for EVFC3PR combined-cycle.*

Fig. 9 shows the variation of CO_2 emission per unit plant output of EVFC3PR combined-cycle w.r.to λ_{IT} and $\beta_{comp.}$ A large reduction in CO_2 emission per unit plant output is observed with increase in λ_{IT}upto 6. This is because an increase in $\lambda_{IT}$is obtained as a result of increase in $T_{i,T}$ and a decrease in $T_{i,C}$, both of which increases η_{plant} and help in a better utilization of fuel. Beyond a λ_{IT} of 6 however, the reduction in coolant flow due to lower $T_{i,C}$ is unable to offset the rise in coolant flow requirement due to higher $T_{i,T}$ resulting in a rise in heat rate and corresponding increase in CO_2 emission per unit plant output.

The variation of CO_2 emissionper unit plant output with β_{comp} however is marginal as the increase in β_{comp} has no considerable effect on heat rate reduction.

4.9 *Variation of cost rate of environmental impact due to CO_2 emission with β_{comp} and $T_{i,T}$*

Fig. 10 shows the effect of β_{comp} and $T_{i,T}$ on environmental impact due to CO_2 emission in terms of the total cost of pollution damage ($/h) by multiplying its flow rate to its corresponding unit damage cost, (C_{CO_2} = 0.024$/kg) [25]. The mass flow rate of air is assumed as 542kg/s [19]. It has been observed that the cost rate of environmental impact due to CO_2 emission reduces significantly with increase in $T_{i,T}$. This is primarily because of enhanced efficiency, reduced fuel consumption and corresponding reduction in CO_2 emission for constant net power output. The variation with β_{comp} suggests the existence of an optimum β_{comp} at any $T_{i,T}$ with reference to the minimum cost of pollution damage. This is because for every $T_{i,T}$ the η_{plant} is maximum at a particular value of β_{comp} . This may be attributed to the combined effect of many factors such as increase in the compressor work, fuel and coolant air requirements and increase in gas-turbine work along with increased irreversibilities due to pumping, cooling and mixing.

V. SUMMARY/CONCLUSIONS

If the Summary/Conclusions section is not wanted, delete this heading and text.

Contact Information

Contact details for the main author should be included here. Details may include mailing address, email address, and/or telephone number (whichever is deemed appropriate).

Acknowledgments

If the Acknowledgments section is not wanted, delete this heading and text.

Definitions/Abbreviations

SA	sample abbreviations
UBT	Use borderless table ≤ 3.5 inches wide.
test vector	Don't capitalize term unless an acronym or proper noun.

Appendix

The Appendix is one-column. If you have an appendix in your document, you will need to insert a continuous page break and set the columns to one. If you do not have an appendix in your document, this paragraph can be ignored and the heading and section break deleted.

REFERENCES

[1]. SAE uses the Chicago Manual of Style in formatting references. In the text of the paper the citations are numerically identified using square brackets [1]. Up to four authors should be listed; more than four, et al. should be used after the fourth author is listed. Refer to the SAE Technical Paper Style Guide for formatting of different types of references. Apply the List-Ordered-Numeric style tag to format references. Below are some examples.

[2]. Guo, Q. and Liu, B., "Simulation and Physical Measurement of Seamless Passenger Airbag Door Deployment," SAE Technical Paper 2012-01-0082, 2012, doi:10.4271/2012-01-0082.

[3]. Kunkel, S., Zimmer, T., and Wachtmeister, G., "Friction Analysis of Oil Control Rings during Running-In," SAE Technical Paper 2011-01-2428, 2012, doi:10.4271/2011-01-2428.

[4]. Morgan, R., Scullion, P., Nix, L., Kan, C. et al., "Injury Risk Investigation of the Small, Rear-seat Occupant in Side Impact," SAE Technical Paper 2012-01-0092, 2012, doi:10.4271/2012-01-0092.

[5]. Kimura, Y. and Murakami, M., "Analysis of Piston Friction - Effects of Cylinder Bore Temperature Distribution and Oil Temperature," *SAE Int. J. Fuels Lubr.* 5(1):1-6, 2012, doi:10.4271/2011-01-1746.

[6]. SAE International Surface Vehicle Recommended Practice, "Laboratory Measurement of the Composite Vibration Damping Properties of Material on a Supporting Steel Bar," SAE Standard J1637, Rev. Aug. 2007.